Electron–acoustic phonon interaction in semiconductor nanostructures: Role of deformation variation of electron effective mass

V. I. Pipa,[1,2] N. Z. Vagidov,[1] V. V. Mitin,[1,*] and M. Stroscio[3]
[1]*Department of Electrical and Computer Engineering, Wayne State University, Detroit, Michigan 48202*
[2]*Institute of Semiconductor Physics, Kiev, 252650, Ukraine*
[3]*U.S. Army Research Office, P.O. Box 12211, Research Triangle Park, North Carolina 27709*
(Received 18 June 2001; published 27 November 2001)

We demonstrate that the phonon-induced variation of electron effective mass gives a substantial contribution to the electron–acoustic-phonon interaction in semiconductor nanostructures. Calculations are carried out for electrons in a quantum well (QW) and a quantum wire (QWR) of III-V heterostructure materials. This mechanism gives rise to an interference effect in electron scattering with longitudinal acoustic phonons via the deformation potential and allows the electrons to interact with transverse acoustic phonons. Due to these peculiarities, the additional channel of scattering can either increase or decrease the total scattering rate. For a given semiconductor, the modified scattering constant has been shown to depend on the dimensionality of the electron gas, the size and the shape of the nanostructure, and on the temperature. The scattering constants for intrasubband transitions in QW's and QWR's are different for the electron energy and momentum relaxation. For narrow QW's or flattened QWR's, modification of the commonly used bulk deformation potential interaction at low temperatures originates mainly due to interaction with transverse acoustic phonons. For GaAs QW of 50 Å width, the ratio of the total relaxation rate of the electron energy to that from the bulk deformation potential coupling is about 0.65 for the temperature 4 K and 1.7 for 20 K.

DOI: 10.1103/PhysRevB.64.235322 PACS number(s): 72.10.−d, 63.22.+m, 73.63.−b

I. INTRODUCTION

The most important mechanism of interaction between electrons and acoustic phonons in semiconductors is the interaction via the deformation potential (DP). In a crystal of the cubic symmetry, the interaction energy of an electron having a wave vector $\mathbf{k}$ close to a conduction-band minimum $\mathbf{k}=0$ is determined by[1] $D(\nabla\cdot\mathbf{u})$ where D is the deformation potential constant and $\mathbf{u}$ is the acoustic displacement. This mechanism leads to the interaction of electrons only with longitudinal acoustic (LA) modes. In a cubic crystal with the energy extremum located at the point $\mathbf{k}\neq 0$ or in anisotropic crystals, the DP interaction is specified by a second-rank tensor, and the electrons interact with transverse acoustic (TA) phonons as well.[2] The bulk DP interaction is widely applied to electrons confined in nanostructures although in crystals having heteroboundaries the translation symmetry is broken. For such structures, the DP constant is treated as an adjustable material parameter differing from the bulk value. In particular, for $Al_xGa_{1-x}As/GaAs$ heterostructures, by matching the theory with the experimental data on electron mobility,[3,4] $|D|\simeq 12$ eV has been obtained while the commonly accepted value for bulk GaAs is 7–8 eV.[5,6] It is usually assumed that scattering of electrons in quantum wells (QW), quantum wires (QWR), and quantum dots with acoustic phonons is described by the same DP constant that does not depend on the size of the nanostructure (e.g., see Ref. 7) and that the coupling constant that determines the energy loss rate is equal to that for the electron mobility.[8,9] The goal of this paper is to reexamine the generally accepted approach according to which the scattering of the confined electrons with acoustic phonons via nonpiezoelectric interactions is specified by a single scattering constant.

In quantum structures, the bulk DP shifts the conduction-band edge and the spatial quantized energies (subbands or discreet levels) at the same value. In structures with small interface spacing, this interaction has to be supplemented by taking into account a direct deformation perturbation of the energy levels.[10–12] The expression for a quantized energy, $E\sim\hbar^2/(m^*L^2)$, indicates that an additional coupling originates from phonon-induced changes of the effective size of electron localization L and the electron effective mass m^*. Our previous analysis[12–14] shows that the main additional size-dependent interaction originates from the deformation-related variation of the effective mass (VEM mechanism). In contrast to bulk materials where VEM mechanism is negligible (for energies near band edge), for nanostructures this interaction can play a noticeable role due to a finite value of the lowest electron energy. If the interface spacing is small enough, electron scattering can be affected strongly by this interaction. The results of calculations briefly reported in Ref. 13 show that the contribution of VEM mechanism to the electron mobility in a narrow GaAs QW is comparable with and can even overcome that from the usual DP coupling. For quantum dots of small sizes, the additional scattering via the VEM mechanism prevents[14] the reduction of the electron relaxation rate with decreasing dot size as predicted by the conventional DP theory.[7]

The additional mechanism brings about qualitatively improved features in the electron-acoustic phonon interaction in low-dimensional structures. First of all, the matrix elements of transition for electron scattering with LA phonons via the DP and VEM interactions appear to be in phase. As a result, the transition probability depends on the sign of the DP constant D. In cubic crystals with the conduction-band minimum at the Γ point, electrons interact with TA phonons as well. Due to the interaction with TA phonons and the interference

effect, the additional mechanism can either augment or suppress the total scattering rate with respect to the rate provided by solely DP coupling.[13,14] The transition probabilities calculated within the framework of the deformation-potential formalism are proportional to the scattering constant D^2. In this paper we show that due to the additional VEM mechanism, the effective scattering constant for the same semiconductor depends on the size and the shape of nanostructure and on the temperature. Moreover, the constants responsible for the electron energy and momentum relaxation appear to be different.

We investigate the influence of the deformation-related variation of the electron effective mass on scattering of QW's and QWR's. We will be interested primarily in nanostructures with electrons completely confined to the interior (the well or the wire). In such structures, the influence of the VEM mechanism can be significant and the electron-acoustic phonon coupling is specified by only two material parameters—a bulk DP constant and the pressure-dependence coefficient of the electron effective mass. Moreover, this allows us to separate the electron motion in all three spatial directions and, thus, to perform an analytical investigation of the associate additional channel of scattering in nanostructures of different shapes. Penetration of electrons into barriers can be regarded as an increase of the effective sizes of nanostructure. It is clear that in this case the partial contribution of the finite-size mechanism decreases. Besides, in order to describe the electron-phonon interaction in a finite-barrier structure, one needs also to know the previously mentioned parameters for barrier materials. For such structures, we will estimate a role of VEM mechanism neglecting a difference in parameters of materials forming nanostructures.

In this study, we concentrate on the role of the VEM mechanism in modifying the kinetic properties of confined electrons. In Sec. II, we introduce the interaction Hamiltonian and estimate a pressure coefficient of the electron effective mass for typical III-V materials. Then, in Sec. III and Sec. IV we evaluate and analyze a contribution of the additional interaction to the electron energy and momentum relaxation due to intrasubband scattering in QW's and QWR's. Principal conclusions of this work are given in Sec. V.

II. BASIC EQUATIONS

In bulk semiconductors, the interaction Hamiltonian associated with a deformation variation of the electron effective mass is well known.[2] For low-dimensional systems, the corresponding perturbation has been derived[13,14] using the kinetic-energy operator of the Ben Daniel-Duke form,[15] $(-\hbar^2/2)\nabla\cdot[m^{-1}(\mathbf{r})\nabla]$. The energy of interaction between electron and the lattice deformation originates from the linear term of an expansion of the inverse effective mass, $1/m(\mathbf{r})$, over the components of the strain tensor. For cubic crystals, we get

$$H=-\frac{\hbar^2}{2}\sum_{\alpha}\nabla_{\alpha}\left(\frac{\chi}{m^*}u_{\alpha\alpha}\nabla_{\alpha}\right), \tag{1}$$

where $\alpha=x$, y, or z, $u_{\alpha\alpha}$ is the diagonal component of the strain tensor, and χ is a phenomenological parameter. The perturbation of Eq. (1) holds for all nanostructure types. For QW's and QWR's, we will disregard the VEM for the directions along which the translation symmetry is preserved. For a weak deformation as in the conventional case of acoustic phonons, the total interaction is defined by a superposition of the deformation-potential interaction and the perturbation of Eq. (1). The parameter χ is expressed through a pressure coefficient of the electron effective mass as $\chi=(3K/m^*)(dm^*/dP)\simeq(3K/E_g)(dE_g/dP)$, where K is the modulus of the hydrostatic compression. The last approximation holds for narrow-gap semiconductors where a linear relationship between m^* and the band-gap energy E_g is satisfied. For a low pressure, the electron effective mass increases with the pressure rise as in the case of the band-gap variation;[16] i.e. $\chi>0$. Using the data for the elastic moduli and pressure coefficients of E_g given in Ref. 16, we find $\chi\simeq 17$ for GaAs, $\chi\simeq 28$ for the $In_{0.53}Ga_{0.47}As$ ternary compound, and $\chi\simeq 42$ for InAs (for InAs, the pressure coefficient of the spin-orbital splitting and the band gap are taken to be equal). For GaAs, the measured pressure coefficient,[17] $dm^*/dP=0.007m^*/\text{kbar}$, corresponds to $\chi\simeq 16$. The inequality $\chi\gg 1$, which holds for the previously considered semiconductors, implies the condition that the additional interaction[10,11] attributed to the phonon-induced changes of the distance between interfaces is small, compared to the VEM interaction. For semiconductors where a shift of conduction-band edge provides the main contribution to the pressure dependence of E_g (this is true for practically all semiconductors[6]), we get $\chi\simeq -3D/E_g$. This relationship shows that $D<0$ and provides an estimate of χ values, which is in acceptable agreement with previously obtained values when $D\simeq -8.1$, -7, and -5.7 for GaAs, $In_{0.53}Ga_{0.47}As$, and InAs, respectively.

We will ignore the effect of acoustic mismatch at the interfaces and use the standard expansion of the displacement $\mathbf{u}$ over the bulk acoustic modes that are found in the isotropic continuum approximation. The differences in elastic constants for the III-V materials forming conventional heterostructures are small[16] and approximation of the same acoustic phonons in the nanostructure and in its matrix is well established.[15] Based on the same elastic constants, the continuum approximation can be used without limitation on the nanostructure size. The probability of a transition between the initial i and the final f electron states is calculated in the first order of perturbation using the Fermi golden rule

$$W_{if}^{\pm}=\frac{2\pi}{\hbar}\sum_{j,\mathbf{q}}\left(\frac{\hbar}{2\rho V\omega_j}\right)|M_{if}^{j,\pm}|^2\left[N\left(\frac{\hbar\omega_j}{k_BT}\right)+\frac{1}{2}\pm\frac{1}{2}\right]\times\delta(\varepsilon_f-\varepsilon_i\pm\hbar s_j q). \tag{2}$$

Here ρ is the density of crystal, V is the normalization volume, and $M_{if}^{j,\pm}$ is the matrix element of the transition; ω_j and $\mathbf{q}$ are the phonon frequency and wave vector, $j=l$ and $j=t_{1,2}$ label longitudinal and two transverse phonon modes, respectively, and N is the Planck distribution function. In Eq. (2) and throughout the remainder of this paper the

upper sign corresponds to emission and the lower sign to absorption of the acoustic phonons. We use a linear isotropic relation $\omega_j = s_j q$ where the sound velocities in a cubic crystal s_j are taken to be equal to the appropriate average quantities.[18] The unit vectors of the phonon polarization $\mathbf{e}_j$ are chosen in the following form:

$$\mathbf{e}_l = \mathbf{q}/q, \quad \mathbf{e}_{t1} = (q_x q_z, q_y q_z, -q_\parallel^2)/q q_\parallel,$$

$$\mathbf{e}_{t2} = (q_y/q_\parallel, -q_x/q_\parallel, 0), \tag{3}$$

where $\mathbf{q}_\parallel = (q_x, q_y, 0)$ and $q_\parallel = \sqrt{q_x^2 + q_y^2}$.

III. QUANTUM WELL

We consider rectangular QW of an infinite length in the x,y directions. Electrons confined in z-direction have two-dimensional wave vector $\mathbf{k} = (k_x, k_y)$ and the energy $E_{1z} + \varepsilon(k)$, where E_{1z} is the lowest energy level of size quantization and $\varepsilon(k) = \hbar^2 k^2/(2m^*)$ is the kinetic energy of electron. We take into account the deformation modulation of the electron effective mass in z direction. For the double-barrier heterostructures under consideration, we also take into account the ''macroscopic deformation potential''[10] associated with the deformation-related change of the interface spacing. This interaction is expressed through a confinement potential $V(z)$ as[12] $-u_z dV/dz$. So, only l and $t1$ modes, which have displacements with $u_z \neq 0$, contribute to the additional mechanisms of electron–acoustic-phonon interaction. Let us consider the intrasubband transitions between the electron states $\mathbf{k},\mathbf{k}'$ in an infinitely deep rectangular QW bounded by planes $z=0$ and $z=L_z$. We obtain $M^{j,\pm}_{\mathbf{k},\mathbf{k}'} = M_j F_{1j} \delta_{\mathbf{k}',\mathbf{k}\mp\mathbf{q}_\parallel}$, where

$$M_l = i q_l [D + (q_{zl}/q_l)^2 D_z(q_{zl})],$$

$$M_t = -i(q_{zt} q_\parallel / q_t) D_z(q_{zt}), \tag{4}$$

where $q_j = \omega/s_j$, $Q_{zj} = q_{zj} L_z/2$, and $E_{1z} = \pi^2\hbar^2/(2m^* L_z^2)$. The electron form factor F_{1j} and the function $D_z(q_z)$ are given by

$$F_{1j} = \frac{2}{L_z}\int_0^{L_z} dz e^{i q_{zj} z} \sin^2\left(\frac{\pi z}{L_z}\right) = \frac{\pi^2 \sin Q_{zj}}{Q_{zj}(\pi^2 - Q_{zj}^2)} e^{i Q_{zj}}, \tag{5}$$

$$D_z(q_z) = E_{1z}\left[\chi - 2 - (\chi - 1)\frac{q_z^2 L_z^2}{2\pi^2}\right]. \tag{6}$$

The previously obtained matrix elements can be derived using the interaction energy, $\Sigma_\alpha D_{\alpha\alpha} u_{\alpha\alpha}$, where the nonzero components of the DP tensor are $D_{xx} = D_{yy} = D$ and $D_{zz} = D + D_z(q_z)$. The symmetry of this tensor reflects the axial symmetry of the QW structure. Separating the bulk potential, one can rewrite this modified DP interaction as $D(\boldsymbol{\nabla}\cdot\mathbf{u}) + D_z u_{zz}$.

Kinetic properties of electrons in QW's subjected to scattering with acoustic phonons via deformation and piezoelectric potentials are described by Price's theory;[19] more detailed calculations were carried out in Ref. 20. In order to illustrate the role of the additional scattering, we calculate the electron energy and momentum relaxation rates, ν_e and ν_m, respectively. We will assume that the electrons are degenerate, i.e., $k_B T \ll \varepsilon_F$, where ε_F is the electron Fermi energy, and the electron temperature T_e deviates slightly from the lattice temperature T. The rate ν_e that relates the electron power loss (per electron) Q with the difference $T_e - T$, as $Q = -\nu_e k_B (T_e - T)$, is given by

$$\nu_e = \frac{m^{*2}}{4\pi^3 n_2 \rho \hbar (k_B T)^2} \times \sum_j \int_0^{\pi/2} d\theta \int_0^\infty d\omega \frac{\omega^3 |M_j|^2 |F_{1j}|^2}{q_{zj} s_j^2 \sinh^2\left(\dfrac{\hbar\omega}{2k_B T}\right)}, \tag{7}$$

where $q_{zj} = [\omega^2/s_j^2 - (2k_F \sin\theta)^2]^{1/2}$, $k_F = (2m^*\varepsilon_F)^{1/2}/\hbar$, 2θ is the angle between the electron's initial and final momenta, and $n_2 = k_F^2/2\pi$ is the sheet density of electrons. The variable ω is expressed through the energy transfer of the electrons as $\omega = |\varepsilon - \varepsilon'|/\hbar$.

Let us first consider the Bloch-Grüneisen regime when the scattering processes are substantially inelastic. This regime corresponds to the temperatures T that are less than or comparable to the characteristic temperature $T_0 = 2 s_t \hbar k_F / k_B$. For this regime, the inequality $q_{zj} L_z \ll 1$ is satisfied, and one can set $F_{1j} = 1$ and $D_z(q_z) = D_z(0)$. In the limiting case of $T \ll T_0$, the above expression for ν_e reduces to

$$\nu_e = \frac{15\zeta(5)\sqrt{2m^*} D_e^2 (k_B T)^4}{\pi \hbar^4 \rho s_l^4 \varepsilon_F^{3/2}}, \tag{8}$$

where $\zeta(x)$ is the Riemann's ζ function and D_e is the renormalized DP constant, which is given by

$$D_e = D\left\{1 + \delta + \left[3 + \left(\frac{s_l}{s_t}\right)^4\right]\frac{\delta^2}{8}\right\}^{1/2}, \quad \delta = (\chi - 2)\frac{E_{1z}}{D}. \tag{9}$$

Equation (8) with D_e determined by $D = \Xi_d$ and $\delta = \Xi_u/\Xi_d$ formally coincides with the rate of energy losses calculated in Ref. 21 for Si metal-oxide-semiconductor field-effect transistors using the deformation-potential interaction $\Xi_d(\boldsymbol{\nabla}\cdot\mathbf{u}) + \Xi_u u_{zz}$. Thus, in a semiconductor with the conduction-band extremum at Γ point, the low-temperature energy relaxation of electrons in a QW due to scattering on acoustic phonons is described by a tensor of deformation potential that takes place for many-valley semiconductors. In our case, a deformation potential related to shear deformation emerges from the additional interaction: $\Xi_u = (\chi - 2) E_{1z}$.

The average momentum relaxation rate of electrons in a QW, ν_m, can be obtained straightforwardly from Eq. (7) by multiplying the integrand by $2k_B T k_F^2 \sin^2\theta/(m^*\omega^2)$. This rate determines the acoustic-phonon-limited electron mobility as $e/(m^*\nu_m)$ (e is charge of the electron). In the limit as T

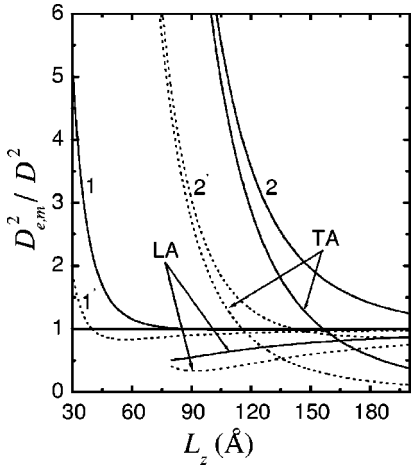

FIG. 1. Ratio of effective coupling constants, D_e^2 and D_m^2, that determine the electron energy and momentum relaxation rates, respectively, to the bulk value D^2 versus the width of quantum well. Solid lines correspond to D_m^2/D^2, dotted lines to D_e^2/D^2; (1),(1′) GaAs ($D=-8$ eV, $\chi=17$); (2), (2′) TA, LA-InAs ($D=-5.8$ eV, $\chi=42$). The curves TA and LA illustrate contributions of transverse and longitudinal phonons.

$\rightarrow 0$, this rate obeys the dependence T^5, valid for deformation-potential scattering,[19] and is specified by the coupling constant

$$D_m = D\left\{1+\frac{\delta}{2}+\left[1+\left(\frac{s_l}{s_t}\right)^6\right]\frac{\delta^2}{8}\right\}^{1/2}, \qquad (10)$$

which differs from D_e. So, in order to describe electron scattering in a QW in the framework of deformation-potential theory, one should not use only one but two adjustable constants—one for the energy losses and another for the electron mobility. The ratio of the scattering constants to the bulk value, $(D_e/D)^2$ and $(D_m/D)^2$, as the functions of QW width L_z are shown in Fig. 1 for GaAs and InAs-based heterostructures (dependences for InAs are shown only for wide QW's where the electron states satisfy the two-band model). We can see that the renormalization of the DP constant is more pronounced in semiconductors with small electron effective masses. The electron momentum relaxation is more affected by the additional scattering than the energy relaxation: D_m^2 exceeds D^2 and increases with the decreasing values of L_z, while the constant D_e^2 varies nonmonotonically and, over a wide range of L_z, deviates slightly from D^2. It is worth emphasizing an important role of TA phonons in electron scattering at low temperatures. Curves TA show that the enhancement of the electron relaxation is caused mainly by scattering at TA phonons. On the contrary, due to the interference effect between the DP and VEM mechanisms, the additional scattering on LA phonons leads to the suppression of the total rate. This peculiarity is illustrated by the sections of the curves $1',2'$ for which $D_e^2<D^2$ and by the curves LA. Note, that an interaction strength smaller than the theoretical calculation of the DP interaction has been observed for electron energy losses in Si heterostructure.[21]

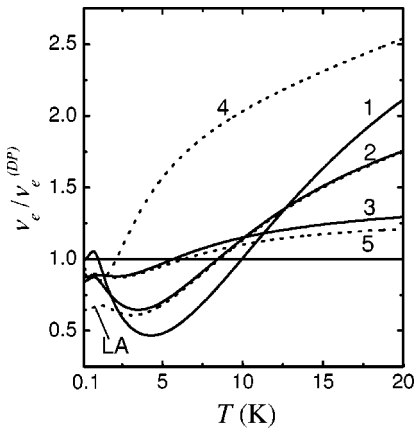

FIG. 2. Normalized electron energy relaxation rates as a function of the temperature for the GaAs (1–3), InAs (4) quantum wells, and for the finite-barrier $In_{0.53}Ga_{0.47}As$ quantum well (5). The width of quantum well: (1) 40 Å ; (2), (5) 50 Å; (3) 80 Å; (4) 150 Å. The electron density: $n_2=2\times10^{11}$ cm^{-2}.

Equations (9) and (10) obtained in the limit $T\rightarrow 0$, become invalid as the temperature increases. With increasing T, phonons with $q_z>q_\parallel$ begin to dominate in the scattering. So far as $M_t\sim q_\parallel$, the contribution of TA phonons decreases. At the same time, due to the change of the sign of $D_z(q_{zl})$ in M_l the additional scattering at LA phonons starts to increase the total rate. This complicated situation (T is of the order or greater than T_0) must be investigated numerically. The temperature dependences of the normalized relaxation rates calculated for various semiconductor materials (Ref. 22) are shown in Figs. 2 and 3. The ratios $\nu_e/\nu_e^{(DP)}$ and $\nu_m/\nu_m^{(DP)}$ can be considered as the normalized effective scattering constants, which depend on the temperature. For $T\rightarrow 0$, they approach to the previously discussed values, $(D_e/D)^2$ and $(D_m/D)^2$, respectively. We see that the interaction via VEM mechanism slows down the electron energy relaxation at low temperatures and accelerates it at high temperatures. On the contrary, the relaxation of electron momentum becomes faster at low T and slower at high T. Comparing curves 2 and

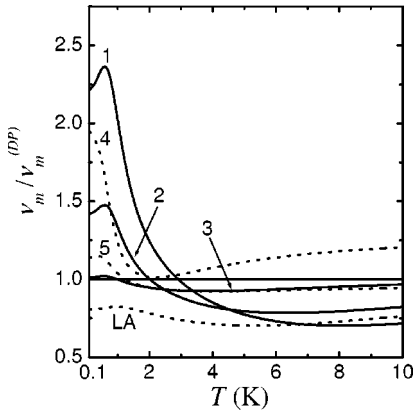

FIG. 3. Normalized momentum relaxation rates of electrons in quantum wells. The notations are the same as in Fig. 2. The curve LA corresponds to the data presented by curve 2 with the scattering on TA phonons disregarded.

LA in Fig. 3, one can see that augmentation of the relaxation rate in the low-T range originates from the scattering with TA phonons.

Certainly at high T, in contrast to the above case of $T \to 0$ illustrated by Fig. 1, the influence of the additional channel of scattering is more pronounced for the electron energy relaxation. Moreover, with increasing T, the rate $\nu_e(T)$ does not tend to saturation as $\nu_e^{(DP)}(T)$ does.[19] This peculiarity originates from the nonlocal nature of the interaction given by Eq. (1). For high T when the inequalities $q_z \gg q_\parallel, L_z^{-1}$ are satisfied, the function $\omega^3 |M_l|^2 |F_{1l}|^2 / q_{zl}$ in Eq. (7) increases as $\omega^2 \sin^2(\omega L_z / 2 s_l)$ with increasing ω while for DP scattering it decreases as $\sin^2(\omega L_z / 2 s_l)/\omega^2$. This represents the unusual situation where the reduction of the electron momentum space dimensionality (described by the electron form factor F_{1l}) does not restrain the electron scattering at short-wavelength phonons. The contribution of such phonons is restricted only by the phonon-distribution function. On the contrary, the influence of VEM mechanism on the momentum relaxation weakens with increasing T. For this relaxation process, the electron collisions with short-wavelength phonons occur under the phonon equipartition distribution ($\hbar\omega \ll k_B T$) and the contribution of such phonons is restricted by the electron form factor. It results in the usual high-temperature asymptote $\nu_m(T) \simeq \nu_m^{(DP)}(T) \sim T$. The set of curves 1–3 in Figs. 2 and 3 show that for GaAs QW's the corrections related to the VEM mechanism become important when the width does not exceed 80 Å .

IV. QUANTUM WIRE

We consider electrons occupying the lowest subband of a rectangular QWR of infinite length in z direction having a y-directed width L_y and an x-directed width L_x (let it be $L_x \leqslant L_y$). Assuming that the potential walls are impenetrable for electrons, we can present the effective-mass electron wave functions in the multiplicative form as

$$\psi = \frac{2}{\sqrt{L_x L_y L_z}} \sin\left(\frac{\pi x}{L_x}\right) \sin\left(\frac{\pi y}{L_y}\right) e^{ikz}, \tag{11}$$

where L_z is the normalization length along the axis of the wire. The electron energy is $E_{1x} + E_{1y} + \varepsilon(k)$, where $E_{1\alpha} = \pi^2 \hbar^2 / (2 m^* L_\alpha^2)$, $\alpha = x, y$, and $\varepsilon(k) = \hbar^2 k^2 / (2 m^*)$. The scattering rate and the transport properties of electrons in a QWR, which interact with acoustic phonons through the deformation potential, were calculated in Refs. 23 and 24. Here, we focus on the role of the additional mechanisms of Eq. (1) in intrasubband scattering of electrons in QWR's. The probability of electron transitions from the initial state k to the final state k' with the assistance of jth acoustic-phonon mode is given by Eq. (2) where now $M_{k,k'}^{j,\pm} = M_j F_{2j} \delta_{k', k \mp q_z}$. Here, $F_{2j} = F_{1j}(Q_x) F_{1j}(Q_y)$ where $Q_\alpha = q_\alpha L_\alpha / 2$. From the energy and momentum conservation it follows[23,24] that for the accepted range of the lowest electron energies ($\varepsilon < m^* s_l^2$), the longitudinal component of the phonon wave vector q_z is much smaller than the transverse component $q_\perp = \sqrt{q_x^2 + q_y^2}$. For GaAs it holds for $\varepsilon(k) > 0.01$ meV. Neglecting the q_z component in the phonon dispersion laws, we get

$$M_l = i q_\perp (D + D_x \cos^2\phi + D_y \sin^2\phi),$$

$$M_{t1} = i q_{zt} (D_x \cos^2\phi + D_y \sin^2\phi),$$

$$M_{t2} = i q_\perp (D_x - D_y) \cos\phi \sin\phi, \tag{12}$$

where ϕ is an azimuth angle in the polar system ($q_x = q_\perp \cos\phi, q_y = q_\perp \sin\phi$) and

$$D_\alpha(q_\alpha) = \chi E_{1\alpha} \left(1 - \frac{q_\alpha^2 L_\alpha^2}{2\pi^2}\right), \quad \alpha = x, y. \tag{13}$$

The matrix elements of Eq. (12) correspond to the following components of the modified DP tensor: $D_{xx} = D + D_x, D_{yy} = D + D_y, D_{zz} = D$. In the general case, all these three components are different.

Some important peculiarities of the electron-acoustic-phonon interaction associated with the VEM mechanism can be revealed from the analysis of the dependence of scattering rate on the electron kinetic energy ε. For the rates of phonon emission, $\nu^{(+)} = \Sigma_{k'} W_{kk'}^{+}$, and absorption, $\nu^{(-)} = \Sigma_{k'} W_{kk'}^{-}$, upon the integration over q_z we get

$$\nu^{(\pm)}(\varepsilon) = \frac{1}{4\pi^2 \rho \hbar} \left(\frac{m^*}{2}\right)^{1/2} \times \sum_j \int_0^{2\pi} d\phi \times \int_0^{q_j^{\pm}} \frac{dq_\perp |M_j|^2 |F_{2j}|^2}{s_j \sqrt{\varepsilon \mp \hbar s_j q_\perp}} (N + 1/2 \pm 1/2), \tag{14}$$

where $j = l, t2$. (The contribution of $t1$ branch of the transverse mode is negligible due to the inequality $q_z \ll q_\perp$.) For the emission rate, the upper limit of integration equals $\varepsilon / (\hbar s_j)$, this limitation is imposed by the requirement that the expression under the square roots must be positive. For the absorption rate, the integration over $q_\perp$ can be formally extended up to ∞.

For scattering of electrons with small energies ($\varepsilon \ll 2\pi\hbar s_t / L_{x,y}$), one can simplify Eq. (14) setting $F_{2j} = 1$ and neglecting the q-dependent terms in D_x and D_y. In this case, the rates of Eq. (14) are proportional to the effective constant $\tilde{D}^2$, which equals $D^2(1 + \delta)$ for QWR's with a square cross section and D_e^2 of Eq. (9) for the flattened QWR's ($L_x \ll L_y$), where now $\delta = \chi E_{1x} / D$. Assuming also that $\hbar\omega \ll k_B T$, we find the low-energy asymptote of the phonon emission rate

$$\nu^{(+)}(\varepsilon) = \frac{2 \tilde{D}^2 k_B T}{3\pi\rho s_l^4 \hbar^4} \left(\frac{m^*}{2}\right)^{1/2} \varepsilon^{3/2} \tag{15}$$

that for $\tilde{D} = D$ coincides with the rate[23] obtained for the DP interaction. We see that in contrast to the DP interaction, the

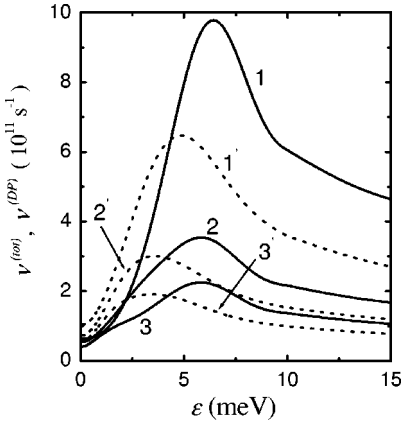

FIG. 4. Total scattering rate (solid lines) and the rate due to DP interaction (dotted lines) versus electron energy for the electron transitions in the lowest subband of GaAs-based quantum wires with the different cross sections: (1),(1′) 50×50 Å^2; (2),(2′) 50 ×100 Å^2; (3),(3′) 50×150 Å^2. $T=20$ K.

phonon emission rate depends on the thickness and the shape of a QWR. For flattened QWR's, as follows from the analysis of D_e for electrons in a QW, the emission of TA phonons appears to be important and the overall rate of phonon emission can be smaller than the rate of LA-phonon emission via solely DP coupling. When the width L_x is less than some critical value, the emission of TA phonons dominates over LA-phonon emission. As seen from Eq. (12), in QWR's that have a square-shaped cross section, TA phonons are not involved in scattering on low-energy electrons.

The electron scattering rate [the sum of the phonon emission and absorption rates calculated from Eq. (14)] as a function of electron energy is shown in Fig. 4 for the three different cross sections of the QWR. For comparison we have also plotted the scattering rates corresponding to the DP interaction. All pairs of curves that correspond to QWR of the same width, e.g., curves 1 and 1′, demonstrate that the VEM mechanism decreases the scattering rate in the low-energy range, shifts the maximum of the spectrum, and increases the rate for electrons with high energies. The first peculiarity appears to be due to the interference effect. The shift of the maximum and increase of the scattering rate at high energies reflect the nonlocal nature of the interaction of Eq. (1): the dependence of the matrix elements on phonon wave vector, presented by Eqs. (12) and (13), prevents the rapid reduction of the scattering rate.

The change of the transition probability modifies both the energy and the momentum relaxation of electrons. To illustrate the role of the VEM mechanism in transport properties of a QWR, we will analyze as in the case of a QW, the average electron energy and momentum relaxation rates. These values are derived from the corresponding balance equations under conditions of a small deviation from equilibrium. As well as for a QW, we use the Fermi distribution function with the electron temperature T_e. This assumption supposes that the electron-electron scattering rate greatly exceeds the electron-phonon relaxation rate. Although such distribution function can be a crude approximation, this model makes possible to consider the main qualitative peculiarities brought about by VEM mechanism into the electron-phonon scattering via DP interaction. (The energy losses of electrons in a QWR due to DP interaction were analyzed, using the electron-temperature approximation, in Ref. 7). Transport properties of electrons are described within a linear response to applied electric field. For degenerate electrons, under such assumptions we obtain

$$\left\{ \begin{matrix} \nu_e \\ \nu_m \end{matrix} \right\} = \frac{1}{n_1 L_z k_B T} \sum_{j,k,k'} W^j_{kk'} f_0(\varepsilon)[1-f_0(\varepsilon')] \times \begin{cases} (\varepsilon-\varepsilon')^2/k_B T \\ \hbar^2(k-k')^2/m^*, \end{cases} \tag{16}$$

where $f_0(\varepsilon)$ is the equilibrium Fermi distribution function, $n_1=2k_F/\pi$ is the electron concentration in a QWR. In Eq. (16), we replace the summation over k,k' with the integration over ε and $\omega=|\varepsilon-\varepsilon'|/\hbar$ and take into account the discontinuity of the probability $W^j_{k,k'}$ at $\varepsilon=\varepsilon'$, according to Eq. (2). Since, for degenerate electrons, the energy transfer $\hbar\omega$ is small compared to the Fermi energy and $\hbar k_F/m^* \gg s_j$, we find that $q_{\perp j} \simeq \omega/s_j \gg q_z$. Performing the integration over ε, we obtain the following final expressions:

$$\left\{ \begin{matrix} \nu_e \\ \nu_m \end{matrix} \right\} = \frac{m^*}{4\pi^3 n_1 \rho \hbar k_B T} \times \sum_j \int_0^{2\pi} d\phi \int_0^{\infty} d\omega \frac{\omega |M_j|^2 |F_{2j}|^2}{s_j^2 \sinh^2\left(\dfrac{\hbar\omega}{2k_B T}\right)} \times \begin{cases} 2m^*\omega^2/(\pi^2 n_1^2 k_B T) \\ 1, \end{cases} \tag{17}$$

where $j=l,t2$. It is easy to see from Eq. (17) that at low temperatures, when the long-wavelength phonons dominate in electron scattering [$F_{2j} \simeq 1$ and $D_\alpha(q_\alpha) \simeq D_\alpha(0)$], both the energy and momentum relaxation rates are proportional to the same effective scattering constant, in contrast with the

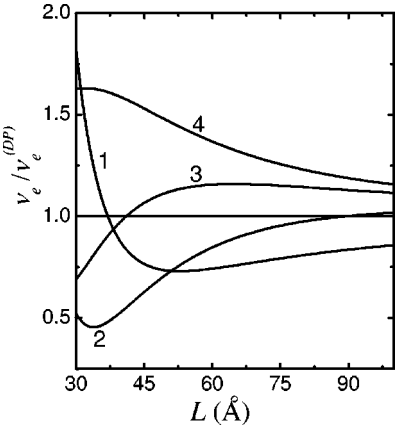

FIG. 5. Normalized electron energy relaxation rates versus the width of GaAs quantum wire with square cross section ($L_x=L_y=L$) for different temperatures T: (1) 1 K; (2) 5 K; (3) 10 K; (4) 15 K.

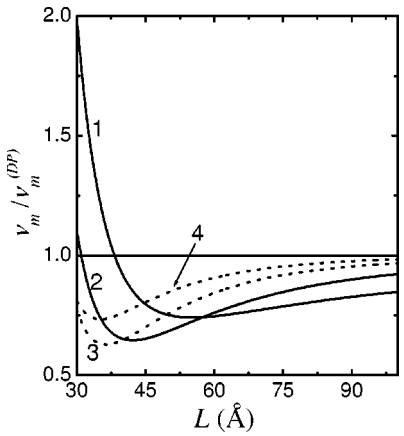

FIG. 6. Normalized electron momentum relaxation rates versus the width of GaAs quantum wire with square cross section ($L_x = L_y = L$) for different temperatures T: (1) 1 K; (2) 5 K; (3) 10 K; (4) 15 K.

case of a QW. This constant coincides with the $\tilde{D}$ value that determines the scattering rate of Eq. (15). With increasing T, when the scattering with short-wavelength phonons becomes important, the ''energy'' and ''momentum'' scattering constants appear to be substantially different. For QWR's with a square cross section, the rates $\nu_e(T)$ and $\nu_m(T)$, normalized at the corresponding rates due to DP coupling, are presented in Figs. 5 and 6 for several temperatures as a function of the width of QWR. As seen, both relaxation rates experience a dual influence as a result of electron scattering on phonons due to the VEM mechanism. As well as for electrons in a QW, the peculiarities appear due to the interference effect in scattering on LA phonons and due to the scattering on TA phonons. Comparing Figs. 5 and 6, one can see that only at low temperatures (curves 1) the ''energy'' and ''momentum'' scattering constants are close to each other. For higher temperatures, these constants differ in magnitude, especially at high T, and have a qualitatively different dependence on the transverse dimensions of the QWR; see curves 4. Figure 5 shows that for QWR's with the same cross section, the scattering constant depends nonmonotonically on the temperature and—for a given temperature—can either decrease or increase with the increasing of thickness of QWR. As seen in Fig. 6, for a narrow electron channel ($L < 40$ Å) and low temperatures, the additional scattering increases the momentum relaxation rate (curve 1), while for the wider channels or higher temperatures it results in a decrease of the rate. Note, that in contrast with the QW case, the effect of TA phonons at low temperatures is less pronounced. Indeed, for QWR's having a square-shaped cross section, the rates given by Eq. (17) are proportional as $T \to 0$ to a scattering constant $D^2(1 + \delta)$ that determines the scattering at LA phonons only. Thus, while electrons in a QW are scattered predominantly on TA phonons, electrons in a QWR with square cross section do not interact with TA phonons at all.

V. CONCLUSIONS

We have studied the role of deformation-induced variations of electron effective mass and the associated contribution of acoustic-phonon scattering to relaxation processes in a low-dimensional electron gas. The electron scattering rates due to interaction of electrons with acoustic phonons via the conventional deformation potential and the VEM mechanism have been calculated for III-V semiconductor QW's and QWR's. The nanostructure-size dependent additional mechanism under consideration brings about qualitatively improved features in the electron-acoustic phonon interaction. It gives rise to an interference effect in electron scattering on LA phonons via the deformation potential and results in the interaction of electrons with TA phonons. We have found that in narrow QW's or thin flattened QWR's, the emission of TA phonons can dominate over the emission of LA phonons under the relaxation of electrons at low temperatures. The interference leads to a dependence of the scattering rate on a sign of the deformation potential constant D. These peculiarities lead to an unusual situation where the additional channel of scattering can either increase or decrease the total scattering rate. In other words, an effective scattering constant that describes the electron relaxation in nanostructures (equals D^2 in the deformation-potential theory) appears to be nonuniversal. For a given semiconductor, the modified scattering constant depends on the dimensionality of the electron gas, the size and the shape of the nanostructure, and on the temperature. We have also demonstrated that one has to use different coupling constants in order to describe the electron energy losses and mobility.

ACKNOWLEDGMENTS

This work was supported by U.S. Army Research Office (Contract No. DAAH04-96-C-0086).

*Corresponding author. FAX: +1-313-577-1101. Email address: mitin@ece6.eng.wayne.edu

[1] J. Bardeen and W. Shockley, Phys. Rev. **80**, 72 (1950); M. F. Deigen and S. I. Pekar, Zh. Eksp. Teor. Fiz. **21**, 807 (1951).

[2] G. L. Bir and G. E. Picus, *Symmetry and Strain Induced Effects in Semiconductors* (Wiley, New York, 1974).

[3] H. L. Störmer, L. N. Pfeiffer, K. W. Baldwin, and K. W. West, Phys. Rev. B **41**, 1278 (1990).

[4] I. Gorczyca and J. Krupski, Phys. Rev. B **52**, 11 248 (1995).

[5] S. Mori and T. Ando, Surf. Sci. **98**, 101 (1998).

[6] Peter Y. Yu and M. Cardona, *Fundamentals of Semiconductors* (Springer-Verlag, Berlin, 1999).

[7] U. Bockelmann and G. Bastard, Phys. Rev. B **42**, 8947 (1990).

[8] S. J. Manion, M. Artaki, M. A. Emanuel, J. J. Coleman, and K. Hess, Phys. Rev. B **35**, 9203 (1987).

[9] A. A. Verevkin, N. G. Ptitsina, G. M. Chulcova, G. N. Gol'tsman, and E. M. Gershenzon, Phys. Rev. B **53**, R7592 (1996).

[10] F. T. Vasko and V. V. Mitin, Phys. Rev. B **52**, 1500 (1994).

[11] P. A. Knipp and T. L. Reinecke, Phys. Rev. B **52**, 5923 (1994).

[12] V. I. Pipa, V. V. Mitin, and M. A. Stroscio, Appl. Phys. Lett. **74**, 1585 (1999).

[13] V. V. Mitin, V. I. Pipa, and M. A. Stroscio, Microelectron. Eng.

47, 373 (1999).
[14] V. I. Pipa, V. V. Mitin, and M. A. Stroscio, Solid State Commun. **117**, 713 (2001).
[15] G. Bastard, *Wave Mechanics Applied in Semiconductor Heterostructures* (Les Editions de Physique, Les Ulis, 1988).
[16] S. Adachi, *Physical Properties of III-V Semiconductor Compounds*: InP, InAs, GaAs, GaP, *and* InGaAs (Wiley, New York, 1992).
[17] G. D. Pitt, J. Lees, R. A. Hoult, and R. A. Stradling, J. Phys. C **6**, 3282 (1973).
[18] S. F. I. Fedorov, *Theory of Elastic Waves in Crystals* (Plenum, New York, 1968).
[19] P. J. Price, J. Appl. Phys. **53**, 6863 (1982); Surf. Sci. **113**, 199 (1982); **143**, 145 (1984).
[20] V. Karpus, Sov. Phys. Semicond. **20**, 6 (1986); **21**, 1180 (1987); **22**, 268 (1988); Semicond. Sci. Technol. **5**, 691 (1990).
[21] R. J. Zieve, D. E. Prober, and R. G. Wheeler, Phys. Rev. B **57**, 2443 (1998).
[22] We use the following $In_{0.53}Ga_{0.47}As$ parameters: $D=-7.2$ eV, $m^*=0.043\ m_0$, $s_l=4.3\times10^5$ cm/s, $s_t=2.3\times10^5$ cm/s, $\rho=5.4$ g/cm^3, and the band-offset 220 meV.
[23] R. Mickevičius and V. Mitin, Phys. Rev. B **48**, 17 194 (1993).
[24] B. K. Ridley and N. A. Zakhleniuk, J. Phys.: Condens. Matter **8**, 8525 (1996); **8**, 8539 (1996); **8**, 8553 (1996).